Genome-wide association study identifies 112 new loci for body mass index in the Japanese population

秋山, 雅人

The contents of this article is now published by *Nature Genetics*:
Akiyama, M. et al. Genome-wide association study identifies 112 new loci for body mass index in the Japanese population. *Nat. Genet.* **49**, 1458–1467 (2017).
https://www.nature.com/articles/ng.3951

DOI number: 10.1038/ng.3951

Genome-wide association study identifies 112 new loci for body mass index in the Japanese population

Authors: Masato Akiyama[1], Yukinori Okada[1,2,3], Masahiro Kanai[1], Atsushi Takahashi[1,4], Yukihide Momozawa[5], Masashi Ikeda[6], Nakao Iwata[6], Shiro Ikegawa[7], Makoto Hirata[8], Koichi Matsuda[9], Motoki Iwasaki[10], Taiki Yamaji[10], Norie Sawada[10], Tsuyoshi Hachiya[11], Kozo Tanno[11,12], Atsushi Shimizu[11], Atsushi Hozawa[13,14], Naoko Minegishi[13,14], Shoichiro Tsugane[15], Masayuki Yamamoto[13,14], Michiaki Kubo[16] and Yoichiro Kamatani[1,17].

Affiliations:

1. Laboratory for Statistical Analysis, RIKEN Center for Integrative Medical Sciences, Yokohama 230-0045, Japan.
2. Department of Statistical Genetics, Osaka University Graduate School of Medicine, Osaka 565-0871, Japan.
3. Laboratory of Statistical Immunology, Immunology Frontier Research Center (WPI-IFReC), Osaka University, Suita, Japan.
4. Laboratory for Omics Informatics, Omics Research Center, National Cerebral and Cardiovascular Center, Osaka 565-8565, Japan.
5. Laboratory for Genotyping Development, RIKEN Center for Integrative Medical Sciences, Yokohama 230-0045, Japan.
6. Department of Psychiatry, Fujita Health University School of Medicine, Aichi 470-1192,

Japan.
7. Laboratory for Bone and Joint Diseases, RIKEN Center for Integrative Medical Sciences, Tokyo 108-8639, Japan.
8. Institute of Medical Science, The University of Tokyo, Tokyo 108-8639, Japan.
9. Graduate school of Frontier Sciences, The University of Tokyo, Tokyo 108-8639, Japan.
10. Division of Epidemiology, Center for Public Health Sciences, National Cancer Center, Tokyo 104-0045, Japan.
11. Iwate Tohoku Medical Megabank Organization, Iwate Medical University, Iwate 028-3694, Japan.
12. Department of Hygiene and Preventive Medicine, School of Medicine, Iwate Medical University, Iwate 028-3694, Japan.
13. Tohoku Medical Megabank Organization, Tohoku University, Sendai 980-8573, Japan.
14. Graduate School of Medicine, Tohoku University, Sendai 980-8575, Japan.
15. Center for Public Health Sciences, National Cancer Center, Tokyo 104-0045, Japan.
16. RIKEN Center for Integrative Medical Sciences, Yokohama 230-0045, Japan.
17. Center for Genomic Medicine, Kyoto University Graduate School of Medicine, Kyoto 606-8507, Japan

Correspondence to: Yoichiro Kamatani (yoichiro.kamatani@riken.jp)

Abstract

Obesity is a risk factor for a wide variety of health problems. By carrying out a genome-wide association study (GWAS) of body mass index (BMI) in Japanese (n = 173,430), we found 85 loci significantly associated ($P < 5.0 \times 10^{-8}$), of which 51 were novel. We conducted trans-ancestral meta-analyses by integrating these results with the results from a GWAS of Europeans, and revealed 61 additional new loci. In total, this study identifies 112 novel loci which double the known BMI loci. By annotating associated variants with cell-type specific regulatory marks, we found the enrichment of variants in CD19+ cells. We also found a significant genetic correlation between BMI and lymphocyte count ($P = 6.46 \times 10^{-5}$, $r_g = 0.18$), and between BMI and multiple complex diseases. These findings provide genetic evidence that lymphocytes were relevant to body weight regulation, and insights into the pathogenesis of obesity.

Introduction

Obesity, which is heritable, is a risk factor for various diseases[1-3]. Thus far, GWASs have identified more than 100 loci associated with BMI [4-7], which is the most commonly used measurement for obesity. However, these loci explained only a small fraction (~3%) of heritability in Europeans[6]. Recent polygenic analyses have suggested that the genetic variants could explain more than 20% of the heritability[6, 8]. Therefore, the majority of the genetic components of BMI have not yet been discovered. Whereas most previous studies were performed using individuals with European ancestry, GWASs in non-Europeans have revealed different loci[5]. Furthermore, epidemiological surveys reported differences in BMI across ethnicities, such as the prevalence of the obese in Asians was lower than that of Caucasians[9]. In addition, Asians tend to develop diabetes with a lesser BMI in comparison with Europeans[10]. These differences imply that investigations in different populations could yield further insights into the etiology of obesity.

To identify genetic loci associated with obesity and to expand the knowledge on body weight regulation, we conducted a GWAS that included >170,000 Japanese subjects (study design is shown in **Supplementary Fig.1**). We then conduct a comprehensive integration with the previous GWAS of Europeans, functional annotations of the associated loci and genetic correlation analyses between BMI and other complex diseases in humans.

RESULTS

Association signals at 85 loci found in Japanese population

For this GWAS, 158,284 Japanese subjects who participated in the BioBank Japan (BBJ) project[11-13] were included. After whole-genome imputation using East Asian (EAS) samples of the 1000 genome project (1KGP)[14] as a reference, we performed a GWAS using 6,108,953 single-nucleotide variants. Although we applied stringent quality controls (QCs), the genomic inflation factor showed remarkable inflation (λ_{GC} = 1.44; **Supplementary Fig. 2a**). To dissect observed inflation into the polygenic effects and potential biases, we performed LD score regression[15]. The estimated mean chi-square and intercept (i.e., the index of biases) values were 1.63 and 1.07 (**Supplementary Fig. 2b**), respectively. These values suggested that polygenic effects induced a majority (89%) of the inflation, and the influence of biases was minimal in comparison with previously reported meta-GWASs[15]. Therefore, we did not apply GC correction to our GWAS.

We observed genome-wide significant (GWS; $P < 5.0 \times 10^{-8}$) levels of association signals at 72 loci (at least 1 Mb apart from each other; **Supplementary Fig. 2c**). We further evaluated 134 lead variants with $P < 1.0 \times 10^{-6}$ using replication sets composed of 15,146 subjects from two independent Japanese population-based cohort studies (the Japan Public Health Center-based Prospective Study (JPHC) and the Tohoku Medical Megabank Project (TMM)). We observed 83% of directional consistency (111 of 134 loci; P for sign test = 5.0×10^{-14}), and all the nominal associations ($P < 0.05$ in the replication sets) were in the same direction (P for sign test = 2.2×10^{-31}). When we combined the results of the GWAS with replication sets, six loci fell below the GWS threshold, whereas 17 additional loci surpassed the GWS level (**Supplementary Table 1** and **2**). Accordingly, 83 loci were significantly associated with BMI (**Supplementary Table 3a, Supplementary Data Set 1** and **2**).

To identify the BMI-associated loci with sex-dependent effects, we performed a

GWAS stratified by sex (**Supplementary Fig. 3**). We identified two male-specific loci that had not been previously reported (rs77511173 and rs111612372, **Supplementary Table 3b**, **4** and **Supplementary Fig. 3c**). We compared the effect sizes of identified variants between sexes; we found that only rs77511173 showed a significant difference ($P_{difference} = 5.88 \times 10^{-5}$, $\alpha = 0.05/ 85$, **Supplementary Table 5** and **Supplementary Fig. 4**). The effect sizes of the variants on the X chromosome were not differed under the assumption of the full dosage compensation ($P_{difference} > 0.05$). We observed nominal differences at two reported sex-dependent loci, *SEC16B*[6] (stronger in females, $P_{difference} = 3.60 \times 10^{-3}$) and *KCNQ1*[5] (stronger in males, $P_{difference} = 3.49 \times 10^{-3}$), but not at other loci (*PCSK1, CDKAL1* and *ALDH2*) [5]. The effect sizes of the associated alleles were strongly correlated between sexes (Pearson's correlation coefficients [r] = 0.92, $P = 5.21 \times 10^{-38}$). We also evaluated the shared heritability between sexes. By applying bivariate LD score regression[16], we observed a significant genetic correlation ($r_g = 0.93$, standard error [SE] = 0.04, $P = 8.3 \times 10^{-151}$), indicating that polygenicity was shared. Taken together, 85 loci, including five loci on the X chromosome and two male-specific loci, were significantly associated with BMI (**Supplementary Table 3**), and 51 were novel.

To assess the robustness, we evaluated the associations of the significant variants in the replication sets. Among them, 49 of 85 (57.6%) were associated with nominal significance ($P < 0.05$). Furthermore, the directions of the effects were consistent at 83 loci (97.6%; P for sign test = 1.89×10^{-22}). We did not find any statistical differences in the number of directionally consistent and nominally associated variants between the previously reported loci and the newly identified loci ($P = 1$ for Fisher's exact test), suggesting that most of the newly identified loci were not false-positives. We observed strong correlation in the effect sizes of associated alleles between the GWAS and the meta-analysis of replication sets ($r = 0.91$, $P = 3.81 \times 10^{-34}$).

Next, we performed a conditional analysis to explore BMI-associated variants independent of the lead variants within the loci. We found four significant second signals that satisfied GWS after conditioning by the lead variants within each region (in a range of ± 1 Mb of each lead variant; **Table 1** and **Supplementary Fig. 5**), and two of these had already been found in Europeans[6] (*GPRC5B*/*GP2* and *NLRC3/ADCY9*). Another two signals were novel secondary associations (*FAM110C/TMEM18* and *HIF1AN-PAX2/BTRC*). Therefore, we determined 89 independent susceptibility variants within 85 loci.

To distinguish association signals found in the Japanese population from those of previously reported by Europeans, we compared the association signals in our GWAS and Europeans by visual inspection, and found three distinct association signals (**Supplementary Fig.6**). When we calculated linkage disequibrium (LD) of 1KGP between lead variants in each GWAS, these variants were in weak LD ($r^2 < 0.02$) in both EUR and EAS. Furthermore, by conditioning on lead variants of Europeans, we confirmed these associations were independent of previously reported ones ($P_{condition} < 5.0 \times 10^{-8}$, **Supplementary Table 6**).

Among the 89 independently associated variants, rs148546399 was low-frequency (minor allele frequency [MAF] ≤ 5%) in East Asian and monomorphic in Europeans, 13 variants had a MAF ≤ 5% in Europeans but common in East Asian (MAF > 5%), and two variants (rs10208649 and rs7903146) were low-frequency in East Asian and common in Europeans according to 1KGP (**Supplementary Table 1** and **4**). When we annotated the variants in LD ($r^2 \geq 0.8$) with the 89 variants reached GWS, we found 29 missense variants (**Supplementary Table 7**), including a missense variant in *GPR101* (rs1190736 [C > A]; NP_473362.1:p.Val124Leu), the causative gene of acromegaly[17]. We additionally evaluated variants in LD with rarer variant rs10208649 (MAF = 1.2 % in EAS), and found the rare coding variant of *GPR75* in moderate LD (rs80328470 [T > C]; NP_006785.1: p.Thr27Ala,

MAF = 0.8 % in EAS; r^2 = 0.66), which is monomorphic in Europeans according to 1KGP and ExAC[18].

We searched the pleiotropy of the 89 identified variants using the GWAS catalog database. We found 32 loci (36%) that had reported associations for other traits (**Supplementary Table 8** and **Supplementary Table 9**). The trait that most frequently overlapped with BMI was type 2 diabetes (T2D; 11.2%), followed by age at menarche (9.0%), and height (6.7%). These overlaps were also observed in Europeans[6].

Identification of 61 new loci through trans-ethnic meta-analyses

To further identify loci associated with BMI, we conducted trans-ethnic meta-analyses using our GWAS and publically available results of Europeans[6] by MANTRA[19]. We first analyzed data sets without sex stratification (N_{max} = 480,438), and observed significant level of the association signals (log_{10} (Bayes' factor) > 6)[20] across 163 loci (**Supplementary Table 10, Supplementary Fig.7** and **Supplementary Data Set 3**). Among them, 54 loci have not been reported (**Table 2**). We note that the previously reported sex-specific loci (*ZBTB10* and *LOC646736*) [6] and an age-dependent locus (*SLC22A3*) [7] reached significant level. We observed 66 of 78 (84.6%) autosomal loci which reached significant level in Japanese and 70 of 91 (76.9%) previously reported loci by the GIANT consortium[6] remained to be significant (variants found by sex-stratified GWAS were excluded). This proportion was not statistically differed between studies (*P* for chi-square test = 0.72). Significant 163 variants showed a significant correlation (r = 0.82, $P = 7.52 \times 10^{-42}$) and directional consistency in the effect sizes between studies (98.8%, $P = 2.28 \times 10^{-45}$; **Supplementary Fig. 8**), indicating BMI associated loci were generally shared across ethnicities. On the other hand, we observed differences in the effect size at 14 loci ($P_{het} < 0.05/163$).

We also performed meta-analysis of sex-stratified GWASs and found six male

specific loci and one female specific locus which had not been reported (**Supplementary Table 11** and **Supplementary Fig.9**). We found distinct but closely located signals in 16q12, where the distances between male-specific rs17795934 and female-specific rs1564981 was less than 1 Mb but in low LD ($r^2 < 0.01$ in both EUR and EAS samples of 1KGP**;** **Supplementary Fig.9c**). Comparison of the effect sizes of the significant variants in this trans-ethnic analysis showed strong correlation between sexes ($r = 0.94$, $P = 1.59 \times 10^{-77}$) with perfect directional consistency (**Supplementary Table 12**), again indicating shared genetic components between sexes.

Using the MANTRA result, we constructed 99% credible sets in each identified locus (**Supplementary Table 13**). When we compared the intervals of the genomic region including variants in the 99% credible set, we observed significant reduction in comparison with the previous trans-ancestral fine-mapping result[6] (*P* for Wilcoxon signed rank test = 0.04; **Supplementary Table 14**). Annotation of the variants included in the 99% credible sets revealed 38 missense variants, including 15 variants found in the Japanese GWAS (**Supplementary Table 15**). Although the majority of the missense variants showed lower posterior probability (PP), we found two likely causal variants with relatively higher PP (KCNJ11, NP_000516.3: p.Val337Ile, PP = 0.75, and HIVEP1, NP_002105.3: p.Met1609Ile, PP = 0.62).

Cell types related to obesity

To investigate specific tissues genetically associated with obesity, we evaluated enrichment of the identified variants included in the 99% credible sets for the cell-type specific active enhancer constructed by the Roadmap project[21] (**Supplementary Note**). After grouping 64 cell-types into 10 categories, we tested for enrichment of the variants, and observed significant enrichment in the active enhancer of the three cell-groups (false discovery rate

[FDR] < 5%; immune related, central nervous system (CNS), and adipose; **Fig.1a, Supplementary Table16** and **Supplementary Table17**). Next, we analyzed each cell-types belonging to immune related and CNS cell-type groups (we only included one cell-type in adipose group). We found that all cell-types belonging to CNS showed significant enrichment (FDR < 5%, 1.23 – 1.68 fold enrichment), whereas B cells was only enriched in immune-related cells (FDR < 5%, 1.60 fold enrichment; **Fig.1b**, **Supplementary Table18**).

Next, we conducted another enrichment analysis using the cell-type-specific trimethylation of histone H3 at lysine 4 (H3K4me3) peaks of 34 cell types using epiGWAS software[22]. Since this analysis requires LD information, we restricted the 84 autosomal variants found in the Japanese GWAS for the analysis. We found three enriched cell types with nominal significance (**Fig. 2** and **Supplementary Table 19**). The cell types were pancreatic islets (P = 0.0013), B cells (CD19+ primary cells, P = 0.0038), and brain (inferior temporal lobe, P = 0.0499). We also applied this method to 97 variants found in the GIANT consortium[6], and found only T cells (CD34+ cells) showed significant enrichment (P = 0.02).

Considering together, our cell-type specificity analyses using the different sets of variants and regulatory markers consistently suggested that B cells, and cells belonging to CNS were relevant to body weight regulation. Although the previous studies highlighted the tissue in the CNS [6, 23], our results imply that gene regulation in immune related cells (B cells and T cells), adipose and pancreas may also have a role in the pathogenesis of obesity. We annotated the lead variants of the identified loci with eQTL[24, 25] in candidate cell-types, and found 69 overlaps (**Supplementary Table 20**).

Variance explained by variants in the GWAS

The lead variants of the 83 identified loci found in Japanese GWAS explained 2.8% of the phenotypic variance (**Supplementary Table 3**), which is similar to that found in Europeans

(2.7% by 97 variants) [6]. Although we included five variants on the X chromosome, which were not analyzed in the GWAS of Europeans, they explained only 0.09% of the phenotypic difference.

To assess the polygenic effects, we estimated the variance explained by all the GWAS variants in the Japanese population-based cohorts using the genomic restricted maximum likelihood (GREML) method implemented in GCTA[26]. The estimated proportion of the phenotypic variance explained by autosomal variants was 29.8 ± 3.4% (mean ± SE). This fraction was similar to that found in the European population (27.4 ± 2.5%) [8]. When we estimated the explained variance of each chromosome[27], a weak linear relationship with chromosome lengths was observed ($P = 7.31 \times 10^{-3}$, $r^2 = 0.30$; **Supplementary Fig. 10**). The X chromosome explained 2.3 ± 0.8% of the phenotypic variance.

We further examined the variance explained in the Japanese cohorts by examining a subset of the variants under a certain *P*-value threshold according to the GWAS results of current Japanese and those of previous Europeans[6] using variants analyzed in both studies. As expected, the explained variance was increased by lowering the threshold of the *P*-value (**Fig. 3** and **Supplementary Fig. 11**). When we compared our GWAS with the GWAS of Europeans, estimates based on our GWAS better explained the phenotypic variance in Japanese cohorts (on average, 1.81 fold higher; range: 1.47–2.17).

Pathway analysis

Using the result of GWAS in the Japanese individuals, we performed MAGENTA[28] to investigate biological pathways associated with obesity and found three significant pathways (ethanol oxidation, glycolysis gluconeogenesis, and maturity-onset diabetes of the young; FDR: $q < 0.05$; **Supplementary Table 21** and **22**). We found that the neurotrophin signaling pathway, which was previously reported in Europeans[6], showed nominal enrichment in our

study (P = 0.0052, q = 0.25).

Stratified analysis by type 2 diabetes

As previous reports suggested that the effect sizes of BMI at a few loci differed between individuals with T2D and individuals who did not develop diabetes (*TCF7L2* (ref. 6) and *CDKAL1* (ref.29)), we evaluated 193 variants by separating GWAS samples into a group of individuals with T2D (n = 31,609) and a group of individuals without diabetes (n = 125,816). We observed significant directional consistency (96.4%, P for sign test = 1.29×10^{-26}) and a significant correlation between the effects (r = 0.85, $P = 8.69 \times 10^{-55}$). Nevertheless, we found evidence of heterogeneity not only at two reported loci but also at five other loci (*HHEX*, *IGFBP2*, *KCNQ1*, *CDKN2B,* and *DUSP9*; α = 0.05/ 193, **Supplementary Fig. 12, 13** and **Supplementary Table 23**). The effects of these variants were stronger in individuals with T2D. Considering that observed effect size of *TCF7L2* in Japanese individuals with T2D (β = 0.12, SE = 0.02) was similar to that in the result of Europeans[6] (β = 0.11, SE = 0.01; $P_{difference}$ = 0.52), some variants may have different impact according to diabetes status.

We also evaluated the effects of BMI-associated variants on T2D susceptibility. Of the 193 variants, we found 20 that showed GWS levels of association for T2D (**Supplementary Table 24**). When we compared the effects of both traits, a bidirectional relationship was observed (**Fig. 4**). A positive relationship was observed at five loci. A negative relationship was found at 15 loci. Although epidemiological studies reported that a higher BMI was a risk for T2D[1], our results indicated that the relationship between genetic variants and T2D susceptibility is more complicated. Of the variants that showed negative relationships, many were reportedly associated with glycemic and/or insulin regulation[30, 31], and insulin processing[31]. Although some loci (*FAM60A* and *FGFR2*) have not been reported to be associated with these traits, this observation implied that they might also share

biological pathways.

To assess the possible biased estimation in our BMI GWAS due to index event bias, we compared the effect sizes for BMI at these loci between GWAS and Japanese population-based cohorts. Among 16 variants which were evaluated in both data sets, we observed a perfect directional consistency and a significant correlation in effect sizes (r = 0.94, $P = 6.63 \times 10^{-8}$; **Supplementary Fig.14**) without significant heterogeneity ($P_{het} > 0.05/16$), suggesting a low possibility of false positive due to case-mix samples in our GWAS.

Genetic correlation analysis

We evaluated the genetic correlation between the results of this study and 33 other GWASs of Asians using bivariate LD score regression[16] (**Fig. 5a**, **Supplementary Table 25** and **Supplementary note**). We found six significant positive correlations (FDR $q < 0.05$), including correlations with T2D, cardiovascular diseases (ischemic stroke, myocardial infarction, and peripheral arterial diseases), asthma, and ossification of posterior longitudinal ligament of the spine (OPLL). Significant negative correlations were observed in adolescent idiopathic scoliosis (AIS), schizophrenia, and rheumatoid arthritis (RA). Genetic correlations with T2D and coronary artery disease have also been reported in Europeans[16]. Other genetic correlations have not been previously reported. To compare our results with that in Europeans, we searched LD hub[32] and found seven results of genetic correlations that were also evaluated in the current study (**Supplementary Table 26**). Similar r_g values were observed between ours and Europeans in the traits reported as significant in our analysis (cardiovascular diseases, RA, schizophrenia, and T2D).

Our cell-type-specific analyses suggested involvement of lymphocytes in the regulation of body weight. Although the genetic involvement of lymphocytes in obesity has

not been elucidated, previous clinical studies have shown positive correlations between BMI and the counts of leukocytes and its subtypes in peripheral blood[33, 34]. We hypothesized that the counts of these cells might be influenced by genetic components that also regulate BMI. We analyzed the genetic correlation between BMI and three major hematological traits (N_{GWAS} = 110,397 - 111,268; **Supplementary Note**) and found a significant positive correlation with white blood cell (WBC) counts ($P = 8.50 \times 10^{-5}$, $r_g = 0.14$; **Fig. 5b** and **Supplementary Table 27**). Next, we evaluated the genetic correlations between BMI and the counts of five WBC subtypes (N_{GWAS} = 63,197). Of these correlations, only lymphocytes showed a significant genetic correlation with BMI ($P = 6.46 \times 10^{-5}$, $r_g = 0.18$). These results implied that BMI and lymphocytes shared genetic components that regulate both traits.

DISCUSSION

Through the largest GWAS of non-European subjects, we found 85 BMI-associated loci, which accounted for ~3% of the phenotypic differences in Japanese subjects. Of the 51 newly identified loci, five were found on the X chromosome and two had sex-dependent effects. Conditional analysis revealed four additional signals within the loci. Furthermore, combining the results with GWAS of Europeans revealed 61 more novel loci, bringing the total number of known susceptibility loci to > 200.

We showed evidence of genetic differences between Europeans and East Asians. First, comparisons of the effect sizes suggested that susceptibility loci were generally shared between Europeans and East Asians, which was compatible with trans-ethnic studies for other traits[35, 36]. On the other hand, variants that were grouped based on the associations of our GWAS were able to explain larger phenotypic differences in Japanese cohorts compared with the variants selected from the GWAS of Europeans. We considered four possible explanation: 1) different causal variants underlie between populations, 2) differences in the effect sizes of causal variants across ethnicities, 3) difference in LD structure between causal variants and GWAS SNPs, 4) differences in allele frequencies of the causal variants. Second, we observed association signals, including second signals, independent of previously reported associations. This could be the result of independent causal variants or distinct LD structures reflecting the same causal variants across ethnicities. Our results emphasize the importance of investigating multiple population to reveal uncovered genetic components. Third, pathway analysis indicated that the neurotrophin signaling pathway influenced BMI across ethnicities, but we also found three pathways that were not reported in Europeans. Considering selection at *ADH1B* and *ALDH2* genes in East Asians[37, 38], the role of the ethanol oxidation pathway and the glycolysis gluconeogenesis pathway, which include both *ADH* and *ALDH* family genes, may have a larger impact on the BMI of East

Asians. These differences highlight the need for the use of diverse populations to better understand the genetic underpinnings of BMI.

Our results suggest two possible ways that lymphocytes are involved in the regulation of body weight. First, gene regulation in B cells might influence body weight regulation because the identified variants were enriched in CD19+ cells-specific chromatin marks. The previous investigation of Europeans using DEPICT suggested candidate genes underlying BMI associated loci were highly expressed in precursor cells B lymphoid and lymphoid progenitor cells[6]. Substantial biological evidence has shown the involvement of immune cells in obesity via inflammation and insulin resistance[39]. Recent studies have also indicated that B cells play an important role in obesity through activation of pro-inflammatory macrophages and T cells and the production of IgG antibodies in insulin resistance[40]. Changes in gene regulation in B cells might affect BMI through these biological mechanisms. Second, the increased number of leukocytes in subjects with obesity[33, 34] might be influenced by genetic variants because we found a significant positive genetic correlation between BMI and counts of WBCs, especially lymphocytes. Our observations indicate that the same genetic variants were increasing (or decreasing) both BMI and counts of these cells. Because genetic correlations could not pinpoint the shared causal variants, further study is needed to elucidate the genetic components of both traits and clarify their underlying biological pathways. Our results provide genetic evidence for the involvement of lymphocytes in the etiology of obesity.

Our cell-type specificity analysis also suggested that cells in pancreatic islets and adipose tissue are relevant to obesity. When we looked up the existing genetic correlations in LD hub[32], significant positive genetic correlations with BMI were found in insulin secretion related measurements (fasting insulin level and HOMA-β) and insulin resistance related trait (HOMA-IR). These facts indicated that BMI shares heritability with insulin modulation. The

previous investigation indicated the enrichment of the BMI heritability in pancreatic islets[23]. Visceral adipose tissue is insulin responsive during obesity, and a major driver of insulin resistance via its chronic inflammation[41]. Furthermore, recent study indicated that the variant at *FTO* region lead *IRX3* and *IRX5* disruption during adipocyte differentiation, and causes body weight gain through cell-autonomous shift from white adipose browning and thermogenesis to lipid storage[42]. Our results may link to these biological knowledge, and suggest that gene regulation in these tissues may influence body weight.

We investigated the genetic correlations between BMI and several other traits and found significant correlations with nine diseases. As we were able to replicate the correlations that were reported in Europeans, genetic correlation may be reproducible across ethnicities. Indeed, a genetic correlation between BMI and schizophrenia was also suggested in Europeans (P = 0.0002, r_g = -0.10)[16]. In observational studies, consistent relationships were found between BMI and T2D, cardiovascular diseases, asthma, OPLL, and AIS[1, 43-45]; however, to our knowledge, the relationships between BMI and RA, and BMI and schizophrenia have been controversial[46-49]. Besides the positive genetic correlation between BMI and T2D, we found some BMI-increasing variants reduce the risk of T2D. Considering T2D confers risk of the multiple diseases, BMI-associated variants may not uniformly influence complex diseases. Our results refine the list of diseases which shares heritability with obesity, and provide insight into the contribution of genetic components in complex diseases.

In conclusion, we performed a large-scale GWAS of BMI and found 112 novel loci. These results highlight that investigating diverse population contributes to identify uncovered loci and to narrow down the candidate genomic region. Our findings provide insight into the links between BMI and complex diseases and provide genetic evidence that lymphocytes play a role in the pathogenesis of obesity.

URLs

BioBank Japan: https://biobankjp.org/english/index.html,

JPHC: http://epi.ncc.go.jp/en/jphc/index.html,

TMM: http://www.megabank.tohoku.ac.jp/english/,

PLINK: https://www.cog-genomics.org/plink2,

MACH: http://csg.sph.umich.edu//abecasis/MaCH/,

EpiGWAS: https://www.broadinstitute.org/mpg/epigwas/,

ANNOVAR: http://annovar.openbioinformatics.org/en/latest/,

SHAPEIT: https://mathgen.stats.ox.ac.uk/genetics_software/shapeit/shapeit.html,

HaploReg: http://www.broadinstitute.org/mammals/haploreg/haploreg.php,

GTEx: http://www.gtexportal.org/home/,

R: https://www.r-project.org/,

MAGENTA: https://www.broadinstitute.org/mpg/magenta/,

GIANT consortium:

https://www.broadinstitute.org/collaboration/giant/index.php/GIANT_consortium,

Locuszoom: http://locuszoom.sph.umich.edu/locuszoom/,

1000 genome project: http://www.1000genomes.org/,

HapMap project: http://hapmap.ncbi.nlm.nih.gov/,

GCTA: http://cnsgenomics.com/software/gcta/,

LDSC: https://github.com/bulik/ldsc/,

GWAS catalog: https://www.ebi.ac.uk/gwas/,

ROADMAP epigenomics PROJECT: http://www.roadmapepigenomics.org/,

LD hub: http://ldsc.broadinstitute.org/

bedtools: http://bedtools.readthedocs.io/en/latest/

Acknowledgments

We would like to acknowledge the staff of the TMM, the JPHC, and the BBJ for collecting samples and clinical information. We are grateful to the staff of the RIKEN Center for Integrative Medical Sciences for genotyping and data management. We thank S. K. Low, K. Suzuki and M.Horikoshi for advice on statistical analyses, and Professor Morris for providing us with the MANTRA software. This study was funded by the BioBank Japan project (M.A., Y.O., M. Kanai, A.T., Y.M., M.H., K.M., M. Kubo and Y.K.) and Tohoku Medical Megabank project (T.H., K.T., A.S., A.H., N.M., and M.Y.), which is supported by the Ministry of Education, Culture, Sports, Sciences and Technology of Japanese government and the Japan Agency for Medical Research and Development. The JPHC Study is supported by the National Cancer Research and Development Fund since 2010, and was by a Grant-in-Aid for Cancer Research from the Ministry of Health, Labour and Welfare of Japan from 1989 to 2010 (M.Iwasaki., T.Y., N.S., and S.T.). GWASs of psychiatric disorders were the results of the Strategic Research Program for Brain Sciences (SRPBS) from the Japan Agency for Medical Research and Development (A.T., M.Ikeda., N.I., M. Kubo and Y.K.).

Author contributions

M.A., Y.K., and M. Kubo conceived and designed the study. K.M., M.H., and M. Kubo collected and managed the BBJ sample. M.Iwasaki, T.Y., N.S., and S.T. collected and managed JPHC sample and information. T.H., K.T., A.S., A.H., N.M., and M.Y. collected and managed the TMM sample. Y.M. and M. Kubo performed genotyping. M.A., M. Kanai, Y.K., and A.T. performed statistical analysis. S.I, M.Ikeda, and N.I. contributed to data acquisition. Y.O., A.T., Y.K., and M. Kubo supervised the study. M.A., Y.O., Y.K., and M. Kubo wrote the manuscript.

Competing financial interests

The authors declare no competing financial interests.

Reference for main text

1) Haslam, D. W. & James, W. P. T. Obesity. *Lancet* **366**, 1197–209 (2005).
2) Wilson, P. W. F., D'Agostino, R. B., Sullivan, L., Parise, H. & Kannel, W. B. Overweight and obesity as determinants of cardiovascular risk: the Framingham experience. *Arch. Intern. Med*. **162**, 1867–72 (2002).
3) Renehan, A. G., Tyson, M., Egger, M., Heller, R. F. & Zwahlen, M. Body-mass index and incidence of cancer: a systematic review and meta-analysis of prospective observational studies. *Lancet* **371**, 569–78 (2008).
4) Speliotes, E. K. et al. Association analyses of 249,796 individuals reveal 18 new loci associated with body mass index. *Nat. Genet*. 42, 937–48 (2010).
5) Wen, W. et al. Meta-analysis of genome-wide association studies in East Asian-ancestry populations identifies four new loci for body mass index. *Hum. Mol. Genet.* **23**, 5492–504 (2014).
6) Locke, A. E. et al. Genetic studies of body mass index yield new insights for obesity biology. *Nature* **518**, 197–206 (2015).
7) Winkler, T. W. et al. The Influence of Age and Sex on Genetic Associations with Adult Body Size and Shape: A Large-Scale Genome-Wide Interaction Study. *PLoS Genetics* **11**, (2015).
8) Yang, J. et al. Genetic variance estimation with imputed variants finds negligible missing heritability for human height and body mass index. *Nat. Genet.* **47**, 1114–20 (2015).
9) Haslam, D. W. & James, W. P. T. Obesity. *Lancet* **366**, 1197–209 (2005).
10) Yoon, K. H. et al. Epidemic obesity and type 2 diabetes in Asia. *Lancet* **368**, 1681–1688 (2006).
11) Nakamura, Y. The BioBank Japan Project. *Clin. Adv. Hematol. Oncol.* 5, 696–7 (2007).
12) Nagai, A. et al. Overview of the BioBank Japan Project: Study design and profile. *J.*

Epidemiol. **27**, 2–8 (2017).

13) Hirata, M. et al. Cross-sectional analysis of BioBank Japan clinical data: A large cohort of 200,000 patients with 47 common diseases. *J. Epidemiol.* **27**, 9–21 (2017).

14) Abecasis, G. R. et al. A map of human genome variation from population-scale sequencing. *Nature* **467**, 1061–73 (2010).

15) Bulik-Sullivan, B. K. et al. LD Score regression distinguishes confounding from polygenicity in genome-wide association studies. *Nat. Genet.* **47**, 291–5 (2015).

16) Bulik-Sullivan, B. et al. An atlas of genetic correlations across human diseases and traits. *Nat. Genet.* **47**, 1236–41 (2015).

17) Trivellin, G. et al. Gigantism and acromegaly due to Xq26 microduplications and GPR101 mutation. *N. Engl. J. Med*. **371**, 2363–74 (2014).

18) Lek, M. et al. Analysis of protein-coding genetic variation in 60,706 humans. *Nature* **536**, 285–291 (2016).

19) Morris, A. P. Transethnic meta-analysis of genomewide association studies. *Genet. Epidemiol.* **35**, 809–822 (2011).

20) Wang, X. et al. Comparing methods for performing trans-ethnic meta-analysis of genome-wide association studies. *Hum. Mol. Genet.* **22**, 2303–2311 (2013).

21) Roadmap Epigenomics Consortium. Integrative analysis of 111 reference human epigenomes. *Nature* **518**, 317–330 (2015).

22) Trynka, G. et al. Chromatin marks identify critical cell types for fine mapping complex trait variants. Nat. Genet. 45, 124–30 (2013).

23) Finucane, H. K. et al. Partitioning heritability by functional annotation using genome-wide association summary statistics. *Nat. Genet.* **47**, 1228–35 (2015).

24) Lonsdale J, et al. The Genotype-Tissue Expression (GTEx) project. *Nat. Genet.* **45**, 580–5 (2013).

25) Westra, H.-J. et al. Systematic identification of trans eQTLs as putative drivers of known disease associations. *Nat. Genet.* **45**, 1238–43 (2013).

26) Yang, J., Lee, S. H., Goddard, M. E. & Visscher, P. M. GCTA: a tool for genome-wide complex trait analysis. *Am. J. Hum. Genet.* **88**, 76–82 (2011).

27) Yang, J. et al. Genome partitioning of genetic variation for complex traits using common SNPs. *Nat. Genet.* **43**, 519–25 (2011).

28) Segrè, A. V, Groop, L., Mootha, V. K., Daly, M. J. & Altshuler, D. Common inherited variation in mitochondrial genes is not enriched for associations with type 2 diabetes or related glycemic traits. *PLoS Genet.* **6**, (2010).

29) Okada, Y. et al. Common variants at CDKAL1 and KLF9 are associated with body mass index in east Asian populations. *Nat. Genet*. **44**, 302–306 (2012).

30) Scott, R. A. et al. Large-scale association analyses identify new loci influencing glycemic traits and provide insight into the underlying biological pathways. *Nat. Genet*. **44**, 991–1005 (2012).

31) Dimas, A. S. et al. Impact of type 2 diabetes susceptibility variants on quantitative glycemic traits reveals mechanistic heterogeneity. *Diabetes* **63**, 2158–71 (2014).

32) Zheng, J. et al. LD Hub: a centralized database and web interface to perform LD score regression that maximizes the potential of summary level GWAS data for SNP heritability and genetic correlation analysis. *Bioinformatics* **33**, 272–279 (2017).

33) Julius, S., Egan, B. M., Kaciroti, N. A., Nesbitt, S. D. & Chen, A. K. In prehypertension leukocytosis is associated with body mass index but not with blood pressure or incident hypertension. *J Hypertens.* **32**, 251–9 (2014).

34) Ilavská, S. et al. Association between the human immune response and body mass index. *Hum. Immunol.* **73**, 480–5 (2012).

35) Okada, Y. et al. Genetics of rheumatoid arthritis contributes to biology and drug discovery. *Nature* **506**, 376–81 (2014).

36) Liu, J. Z. et al. Association analyses identify 38 susceptibility loci for inflammatory bowel disease and highlight shared genetic risk across populations. *Nat. Genet*. **47**, 979–86 (2015).

37) Oota, H. et al. The evolution and population genetics of the ALDH2 locus: Random genetic drift, selection, and low levels of recombination. *Ann. Hum. Genet.* **68**, 93–109 (2004).

38) Han, Y. et al. Evidence of positive selection on a class I ADH locus. *Am. J. Hum. Genet.* **80**, 441–56 (2007).

39) Johnson, A. M. F. & Olefsky, J. M. The origins and drivers of insulin resistance. *Cell* **152**, 673–84 (2013).

40) Winer, D. A. et al. B cells promote insulin resistance through modulation of T cells and production of pathogenic IgG antibodies. *Nat. Med.* **17**, 610–7 (2011).

41) Winer, D. a, Winer, S., Chng, M. H. Y., Shen, L. & Engleman, E. G. B Lymphocytes in obesity-related adipose tissue inflammation and insulin resistance. *Cell. Mol. Life Sci.* **71**, 1033–1043 (2013).

42) Claussnitzer, M. et al. FTO Obesity Variant Circuitry and Adipocyte Browning in Humans. *N. Engl. J. Med.* **373**, 895–907 (2015).

43) Hjellvik, V., Tverdal, A & Furu, K. Body mass index as predictor for asthma: a cohort study of 118,723 males and females. *Eur. Respir. J.* **35**, 1235–42 (2010).

44) Inamasu, J., Guiot, B. H. & Sachs, D. C. Ossification of the posterior longitudinal ligament: an update on its biology, epidemiology, and natural history. *Neurosurgery* **58**, 1027–39 (2006).

45) Tam, E. M. et al. Lower Muscle Mass and Body Fat in Adolescent Idiopathic Scoliosis are Associated With Abnormal Leptin Bioavailability. *Spine* (Phila. Pa. 1976). **41**, 940–6 (2015).

46) Turesson, C., Bergström, U., Pikwer, M., Nilsson, J.-Å. & Jacobsson, L. T. H. A high body mass index is associated with reduced risk of rheumatoid arthritis in men, but not in women. *Rheumatology* (Oxford). **55**, 307–14 (2016).

47) Qin, B. et al. Body mass index and the risk of rheumatoid arthritis: a systematic review and dose-response meta-analysis. *Arthritis Res. Ther*. **17**, 86 (2015).

48) Zammit, S. et al. Height and body mass index in young adulthood and risk of schizophrenia: a longitudinal study of 1 347 520 Swedish men. *Acta Psychiatr. Scand*. **116**, 378–85 (2007).

49) Wyatt, R. J., Henter, I. D., Mojtabai, R. & Bartko, J. J. Height, weight and body mass index (BMI) in psychiatrically ill US Armed Forces personnel. *Psychol. Med*. **33**, 363–8 (2003).

Figure legends for main text

Figure 1. Enrichment of identified variants in active enhancer.

We evaluated enrichment of the variants included in the 99% credible sets for active enhancer. We calculated empirical *P*-values by 1×10^7 permutations, and estimated FDR using Benjamini–Hochberg method. Vertical dashed lines denote FDR = 0.05. (a) Enrichment for active enhancer in 10 cell-groups. (b) Enrichment for active enhancer in immune related cell group and CNS group. We showed the cell-types which showed *P*-values < 0.05. Each bar is colored according to the cell-groups as shown in (a).

Figure 2. Enrichment of identified variants in H3K4me3 peaks.

We analyzed enrichment of identified variants in H3K4me3 peaks of 34 cell types using epi-GWAS software with 1×10^6 permutations. The scale of the X axis corresponds to the *P*-value in the $\log_{10}$ scale for each cell type. The dashed line indicates $P = 0.05$.

Figure 3. Variance explained by subsets of associated variants in Japanese cohorts.

We plotted the estimated variance explained by subsets of variants below the *P*-value threshold from the current Japanese GWAS (red circle) and the GWAS of Europeans (blue circle). Explained variance was estimated from two Japanese population-based cohorts (*N* = 5,612 and 6,434 in the JPHC and the TMM, respectively). Weighted average from two cohorts is shown. Error bars denote the standard error of estimates. Single asterisks indicate significant differences between the explained variance estimated from each study ($P < 0.05$). Double asterisks denote the Bonferroni-corrected level of significance ($P < 0.05/ 7$).

Figure 4. Scatter plot of the effect sizes for BMI and T2D

Effect sizes of 193 identified variants for BMI (X axis) and T2D (y axis). Plots were colored according to the significance level for T2D.

Figure 5. Genetic correlation

Each plot shows the genetic correlation (r_g) between BMI and analyzed traits (a: diseases, and b: hematological traits) estimated from cross-trait LD score regression. Error bars indicate the standard error of estimates. Significant (FDR $q < 0.05$) genetic correlations are colored red and blue for positive and negative relationships, respectively. OPLL: ossification of posterior longitudinal ligament of the spine, PAD: peripheral artery disease, AMD: age-related macular degeneration, AIS: adolescent idiopathic scoliosis, RBC: red blood cell, WBC: white blood cell.

597

Table 1. Result of the condition analysis

SNP	Positional Candidate gene	Chr.	Position[a]	Allele REF/ALT	Crude			Condition		
					beta[b]	s.e.m	P value	beta[b]	s.e.m	P value
rs939584	*FAM150B,TMEM18*	2	621,558	C/T	0.054	0.006	1.39E-19	0.053	0.006	1.55E-18
rs4430979	*FAM110C*	2	47,208	T/G	0.031	0.005	5.40E-10	0.029	0.005	6.32E-09
rs2495707	*HIF1AN,PAX2*	10	102,425,949	A/G	-0.025	0.004	6.21E-09	-0.023	0.004	3.80E-08
rs11191021	*BTRC*	10	103,231,641	A/G	0.021	0.004	8.12E-09	0.020	0.004	4.97E-08
rs2540034	*ADCY9*	16	4,022,694	C/T	0.028	0.004	3.49E-11	-0.029	0.004	1.11E-11
rs7199766	*SLX4*	16	3,637,429	G/A	0.020	0.004	1.25E-07	0.021	0.004	3.95E-08
rs1259768	*GPR139,GP2*	16	20,258,432	C/A	-0.030	0.005	6.80E-11	-0.031	0.005	3.90E-11
rs1011939	*GPRC5B,GPR139*	16	19,992,996	G/A	-0.025	0.004	8.26E-11	-0.025	0.004	4.73E-11

Result of the conditional analysis.

Chr., chromosome; REF, reference allele; ALT, alternative allele.

[a]Positions are based on Build37 (hg19).

[b]Alternative alleles were treated as effective allele.

598

Table. 2 New loci identified by trans-ethnic meta-analyses

SNP	Analysis	Chr.[a]	Position[a] (bp)	Alleles REF/ALT	1KG phase 1 ALT freq		Candidate gene(s)	BBJ GWAS			European GWAS			Trans-ancestral meta-analysis							
															MANTRA				Fixed-effect meta-analysis			
					EAS	EUR		beta[b]	s.e.m	P value	beta[b]	s.e.m	P value	N all	Posterior mean allelic effect	s.e.m	$Log_{10}BF$	$Log_{10}BF$ for heterogeneity	beta[b]	s.e.m	P value	Phet[c]
rs12044597	All	1	1,708,801	A/G	0.47	0.51	*NADK*	0.013	0.004	3.16E-04	0.015	0.003	1.35E-06	474,968	0.014	0.002	7.49	0.05	0.014	0.002	1.54E-09	0.64
rs11185092	All	1	107,886,278	A/G	0.16	0.22	*NTNG1*	0.020	0.005	7.46E-05	0.018	0.005	9.97E-05	392,297	0.019	0.003	6.29	0.07	0.019	0.003	2.89E-08	0.80
rs10923724	All	1	119,546,842	C/T	0.58	0.57	*TBX15,WARS2*	-0.015	0.004	2.89E-05	-0.012	0.003	1.33E-04	480,391	-0.013	0.002	6.28	-0.09	-0.013	0.002	2.34E-08	0.46
rs10754220	All	1	197,244,290	G/A	0.19	0.30	*CRB1*	-0.025	0.005	2.86E-07	-0.013	0.004	1.28E-03	392,262	-0.018	0.003	6.85	-0.02	-0.018	0.003	7.90E-09	0.07
rs823114	All	1	205,719,532	G/A	0.50	0.53	*NUCKS1*	-0.014	0.004	4.51E-05	-0.012	0.003	2.02E-04	473,158	-0.013	0.002	6.12	0.04	-0.013	0.002	4.29E-08	0.53
rs9786986	All	1	235,656,632	G/T	0.49	0.11	*B3GALNT2*	0.016	0.004	4.80E-06	0.020	0.005	7.43E-05	480,088	0.017	0.003	7.28	-0.15	0.017	0.003	1.55E-09	0.60
rs4596023	All	2	48,955,683	A/G	0.66	0.73	*LHCGR,STON1-GTF2A1L*	0.016	0.004	1.14E-05	0.013	0.004	2.84E-04	480,125	0.014	0.003	6.45	-0.14	0.014	0.003	1.50E-08	0.54
rs7569376	All	2	205,385,322	T/C	0.47	0.79	*ICOS,PARD3B*	-0.017	0.004	3.70E-06	-0.015	0.005	2.52E-03	391,110	-0.016	0.003	6.02	-0.04	-0.016	0.003	3.50E-08	0.73
rs972540	All	2	207,244,783	A/G	0.19	0.24	*ZDBF2,ADAM23*	0.013	0.005	7.66E-03	0.018	0.003	2.28E-07	480,378	0.016	0.003	6.77	0.10	0.016	0.003	6.39E-09	0.37
rs7613875	All	3	49,971,514	C/A	0.14	0.52	*MON1A,RBM6*	0.015	0.005	1.50E-03	0.016	0.003	7.36E-07	464,114	0.016	0.003	7.00	-0.08	0.016	0.003	4.38E-09	0.95
rs1225051	All	3	131,645,972	G/A	0.46	0.44	*CPNE4*	0.012	0.004	6.28E-04	0.016	0.004	9.32E-06	392,295	0.014	0.003	6.29	0.13	0.014	0.003	3.11E-08	0.41
rs7621025	All	3	136,272,246	T/C	0.84	0.73	*STAG1*	0.015	0.005	1.77E-03	0.017	0.004	2.80E-06	480,294	0.016	0.003	6.47	0.10	0.016	0.003	2.07E-08	0.72
rs4834272	All	4	113,313,986	T/C	0.53	0.31	*ALPK1*	0.014	0.004	5.33E-05	0.013	0.003	3.71E-05	480,262	0.014	0.002	6.77	0.26	0.014	0.002	1.04E-08	0.83
rs7720894	All	5	60,733,933	G/C	0.39	0.48	*ZSWIM6*	-0.020	0.004	6.12E-07	-0.011	0.004	3.22E-03	392,090	-0.015	0.003	6.20	0.00	-0.015	0.003	2.89E-08	0.10
rs3849724	All	5	173,290,977	G/T	0.25	0.50	*LINC01485,CPEB4*	-0.018	0.004	5.85E-06	-0.014	0.003	9.76E-06	480,165	-0.015	0.003	7.94	-0.02	-0.015	0.002	4.95E-10	0.37
rs2228213	All	6	12,124,855	G/A	0.23	0.33	*HIVEP1*	-0.017	0.004	1.60E-05	-0.016	0.003	1.04E-06	480,386	-0.016	0.003	8.65	0.03	-0.016	0.003	1.03E-10	0.81
rs7779181	All	7	32,345,283	T/C	0.23	0.20	*PDE1C,LOC100130673*	0.015	0.004	2.52E-04	0.019	0.004	2.37E-05	392,261	0.017	0.003	6.32	0.22	0.017	0.003	2.63E-08	0.58
rs10269783	All	7	49,616,203	G/A	0.60	0.37	*CDC14C,VWC2*	0.015	0.004	3.42E-05	0.014	0.003	4.14E-06	477,965	0.015	0.002	7.78	-0.20	0.015	0.002	4.87E-10	0.92

rs3779273	All	7	77,828,940	G/A	0.44	0.40	*MAGI2*	-0.014	0.004	1.18E-04	-0.015	0.003	1.52E-06	480,399	-0.014	0.002	7.66	-0.17	-0.014	0.002	7.55E-10	0.82
rs12156392	All	8	28,140,103	C/A	0.35	0.41	*ELP3,PNOC*	0.019	0.004	6.59E-07	0.011	0.004	5.28E-03	392,039	0.015	0.003	6.16	0.06	0.015	0.003	4.42E-08	0.11
rs10091344	All	8	34,132,075	G/A	0.44	0.34	*DUSP26,LINC01288*	-0.015	0.004	2.21E-05	-0.016	0.004	9.62E-05	392,217	-0.015	0.003	6.80	0.05	-0.015	0.003	8.33E-09	0.93
rs10811901	All	9	23,356,935	G/A	0.86	0.62	*LINC01239,LOC101929563*	0.023	0.004	7.57E-08	0.010	0.003	1.89E-03	461,004	0.015	0.003	6.54	0.11	0.015	0.003	1.26E-08	0.02
rs580809	All	9	101,518,442	C/T	0.56	0.75	*ANKS6*	-0.016	0.004	7.74E-06	-0.012	0.004	6.75E-04	480,376	-0.014	0.002	6.31	0.02	-0.014	0.002	2.70E-08	0.42
rs7024334	All	9	109,072,075	T/G	0.42	0.77	*TMEM38B,MIR8081*	-0.014	0.004	1.55E-04	-0.016	0.004	1.41E-05	473,417	-0.015	0.003	6.53	-0.07	-0.015	0.003	1.14E-08	0.66
rs2270204	All	9	131,042,734	T/G	0.58	0.27	*SWI5*	0.016	0.004	5.47E-06	0.019	0.004	2.60E-07	475,247	0.018	0.003	9.56	-0.12	0.018	0.003	9.02E-12	0.63
rs2163188	All	10	65,314,711	G/C	0.33	0.50	*REEP3*	0.015	0.004	8.63E-05	0.015	0.004	5.03E-05	388,579	0.015	0.003	6.50	0.72	0.015	0.003	1.67E-08	0.99
rs5215	All	11	17,408,630	C/T	0.62	0.66	*KCNJ11*	0.018	0.004	5.33E-07	0.014	0.003	1.13E-05	474,995	0.016	0.002	9.10	0.14	0.016	0.002	3.22E-11	0.34
rs3026401	All	11	31,807,524	C/T	0.52	0.81	*PAX6*	0.016	0.004	3.59E-06	0.016	0.005	8.37E-04	392,284	0.016	0.003	6.56	0.20	0.016	0.003	1.13E-08	0.90
rs506338	All	11	64,440,920	T/C	0.23	0.71	*NRXN2*	0.017	0.005	2.30E-04	0.015	0.003	1.30E-05	480,264	0.016	0.003	6.65	-0.04	0.016	0.003	9.72E-09	0.62
rs11607976	All	11	69,279,111	C/T	0.07	0.30	*MYEOV,LINC01488*	-0.027	0.008	6.54E-04	-0.017	0.003	7.72E-07	479,024	-0.018	0.003	7.01	0.18	-0.018	0.003	3.85E-09	0.25
rs10899469	All	11	78,018,313	T/C	0.41	0.19	*GAB2*	-0.015	0.004	2.51E-05	-0.016	0.004	1.66E-04	477,329	-0.015	0.003	6.46	-0.02	-0.015	0.003	1.49E-08	0.89
rs10772983	All	12	17,141,582	C/T	0.68	0.57	*SKP1P2*	-0.014	0.004	2.42E-04	-0.012	0.003	4.62E-05	478,531	-0.013	0.002	6.18	0.34	-0.013	0.002	3.45E-08	0.73
rs11105839	All	12	91,237,920	T/A	0.48	0.36	*LINC00936,LINC00615*	-0.013	0.004	2.84E-04	-0.013	0.003	2.97E-05	474,917	-0.013	0.002	6.28	0.16	-0.013	0.002	2.54E-08	0.96
rs2321882	All	13	59,451,989	G/C	0.09	0.24	*LOC101926897,DIAPH3*	0.026	0.006	3.60E-06	0.016	0.005	3.64E-04	392,005	0.020	0.004	6.52	-0.07	0.020	0.004	1.32E-08	0.17
rs1927790	All	13	96,922,191	T/C	0.36	0.45	*HS6ST3*	0.010	0.004	5.29E-03	0.015	0.003	7.87E-07	480,335	0.013	0.002	6.15	0.05	0.013	0.002	2.70E-08	0.27
rs12895330	All	14	33,305,343	G/C	0.24	0.49	*AKAP6,NPAS3*	0.020	0.004	6.17E-06	0.016	0.004	1.07E-04	385,665	0.018	0.003	7.18	0.18	0.018	0.003	3.54E-09	0.44
rs709400	All	14	104,149,475	A/G	0.10	0.40	*KLC1*	-0.010	0.005	5.35E-02	-0.017	0.003	1.02E-07	480,397	-0.015	0.003	6.05	-0.40	-0.015	0.003	1.80E-08	0.31
rs12440086	All	15	27,038,492	C/A	0.59	0.54	*GABRB3,GABRA5*	0.017	0.004	3.02E-06	0.012	0.004	1.74E-03	392,170	0.015	0.003	6.21	-0.05	0.015	0.003	3.06E-08	0.33
rs1559677	All	15	47,738,063	A/G	0.43	0.36	*SEMA6D*	0.016	0.004	1.06E-05	0.011	0.003	5.77E-04	480,342	0.013	0.002	6.01	-0.23	0.013	0.002	3.37E-08	0.30
rs9302817	All	16	6,163,936	T/G	0.43	0.18	*RBFOX1*	-0.015	0.004	6.15E-05	-0.019	0.005	1.54E-04	392,179	-0.016	0.003	6.02	0.06	-0.016	0.003	4.56E-08	0.49
rs7200543	All	16	15,129,970	A/G	0.38	0.32	*PDXDC1*	-0.015	0.004	4.16E-05	-0.015	0.003	1.03E-05	480,268	-0.015	0.002	7.44	-0.14	-0.015	0.002	1.24E-09	0.97
rs7195386	All	16	24,578,458	T/C	0.46	0.53	*RBBP6*	-0.016	0.004	6.15E-06	-0.013	0.004	4.89E-04	392,282	-0.015	0.003	6.58	0.38	-0.015	0.003	1.42E-08	0.51
rs2307022	All	16	68,381,978	A/G	0.88	0.65	*PRMT7*	-0.015	0.006	8.15E-03	-0.016	0.003	9.86E-07	480,262	-0.016	0.003	6.26	0.28	-0.016	0.003	3.41E-08	0.83

rs4925114	All	17	17,711,270	A/G	0.07	0.60	*RAI1*	0.029	0.006	1.86E-06	0.014	0.004	5.11E-04	392,169	0.019	0.003	6.26	0.18	0.018	0.003	3.04E-08	0.04
rs4986044	All	17	21,261,560	C/T	0.58	0.49	*MAP2K3,KCNJ12*	-0.013	0.004	3.65E-04	-0.016	0.003	1.42E-07	476,195	-0.015	0.002	8.32	1.22	-0.015	0.002	2.17E-10	0.53
rs12150665	All	17	34,914,787	T/C	0.39	0.40	*GGNBP2*	-0.015	0.004	5.06E-05	-0.016	0.003	2.44E-07	480,289	-0.016	0.002	8.98	0.12	-0.016	0.002	4.67E-11	0.78
rs6504108	All	17	46,292,923	C/T	0.78	0.70	*SKAP1*	-0.019	0.004	1.04E-05	-0.017	0.003	3.58E-07	480,392	-0.018	0.003	9.46	0.06	-0.018	0.003	1.51E-11	0.74
rs9304204	All	18	36,896,003	A/G	0.83	0.81	*LINC00669*	0.017	0.004	4.56E-05	0.018	0.005	2.67E-04	392,282	0.017	0.003	6.03	0.01	0.017	0.003	4.53E-08	0.92
rs4129322	All	18	50,605,642	G/A	0.31	0.10	*DCC*	-0.020	0.004	6.21E-08	-0.011	0.007	1.23E-01	392,300	-0.018	0.003	6.07	0.11	-0.018	0.003	4.23E-08	0.20
rs7243785	All	18	52,475,162	A/G	0.38	0.23	*DYNAP,RAB27B*	0.018	0.004	2.70E-06	0.018	0.004	6.97E-05	382,050	0.018	0.003	7.85	0.01	0.018	0.003	7.79E-10	0.91
rs12454712	All	18	60,845,884	T/C	0.45	0.40	*BCL2*	0.019	0.004	4.79E-07	0.017	0.004	1.46E-05	401,822	0.018	0.003	9.06	-0.09	0.018	0.003	3.26E-11	0.77
rs17710386	All	18	63,461,201	T/C	0.31	0.34	*CDH7*	0.017	0.004	1.94E-05	0.012	0.003	2.26E-04	474,561	0.014	0.003	6.10	-0.13	0.014	0.003	2.77E-08	0.41
rs4805566	All	19	30,918,316	T/A	0.69	0.67	*ZNF536*	0.018	0.004	2.23E-05	0.018	0.004	8.59E-06	389,755	0.018	0.003	7.74	0.01	0.018	0.003	7.88E-10	0.98
rs1884897	All	20	6,612,832	A/G	0.89	0.60	*CASC20,BMP2*	0.014	0.006	2.42E-02	0.016	0.003	6.83E-07	480,315	0.015	0.003	6.12	0.02	0.015	0.003	3.64E-08	0.79

Loci reached genome-wide significance after meta-analysis to European results were shown.

Chr., chromosome; REF, reference allele; ALT, alternative allele; BF, Bayes' factor.

[a]Positions are based on Build37 (hg19).

[b]Alternative alleles were treated as effective allele.

[c]P for heterogeneity between studies estimated by Cochran's Q test.

99

METHOD

Subjects

We used BMI and genome-wide variant data obtained from the BBJ[11-12], which has enrolled approximately 200,000 individuals consisting of 47 various disease[13]. For the GWAS, we set the eligibility criteria as follows: 1) aged ≥ 18, 2) registered height and weight, and 3) individuals whose height was within 3 times of interquartile range (IQR) of upper/lower quartile. For the quality control of GWAS, we excluded samples with a call rate ≤ 0.98. Closely related samples, which were estimated using identity by state (IBS), were excluded by visual inspection. We performed principal component analysis (PCA) for genotype using an in-house program based on the algorithm implemented by smartpca[50], and we excluded outliers from the East Asian cluster. Finally, we calculated the Z-score for height by linear regression using age, sex, status of 47 diseases, and the top 10 principal components (PCs) and excluded individuals out of ± 4 standard deviations (SD) for the purpose of quality control of the phenotype data.

Subjects of the population-based prospective cohorts were independently recruited in the JPHC and the TMM. The inclusion and exclusion criteria for the analysis were the same as for the GWAS. After exclusion of individuals who lacked clinical information including age, sex, height and body weight, we excluded related individuals with PI_HAT > 0.125, which was calculated using PLINK[51]. To calculate the Z-score for height, we used age, sex, and the top 10 PCs as covariates and excluded outliers using the same criterion used in the GWAS. We obtained approval from ethics committees at all collaborating facilities. Informed consent was obtained from all participants before enrollment. Characteristics of the cohorts are shown in the **Supplementary note**.

Phenotype

The BMI information obtained from medical records was standardized using a rank-based inverse-normal transformation. We first calculated residuals for the log-transformed BMI by linear regression analysis using age, age^2, sex, status of 47 registered diseases, and the top 10 PCs as covariates. Then, we transformed residuals using a rank-based inverse-normal transformation. In the cohort studies, linear regression was performed using age, age^2, sex, and the top 10 PCs for the log-transformed BMI in each cohort, and we transformed residuals using a rank-based inverse-normal transformation.

Genotyping and imputation

The subjects of the GWAS were genotyped using the Illumina HumanOmniExpressExome BeadChip or in combination of Illumina HumanOmniExpress and HumanExome BeadChips. We aligned the probe sequence in the manifest files of genotyping array to GRCh37.3 reference using BLAST to convert genotypes into forward strand, and phased haplotypes using MACH[52]. Imputation was performed by minimac (v0.1.1). We used EAS samples of 1KGP (phase1v3) as a reference. We performed quality control on the reference panel as follows: we excluded 11 closely related individuals estimated from IBS, and excluded variants with a minor allele frequency (MAF) < 1.0% and a *P*-value for Hardy–Weinberg equilibrium ≤ 1.0×10^{-6} from the reference panel. After the imputation, we used SNPs with an imputation quality of Rsq ≥ 0.7 for the GWAS.

In the population-based cohorts, DNA samples were genotyped using the Illumina HumanOmniExpressExome BeadChip. We phased haplotypes using SHAPIT[53] (v2.r778) and performed imputation using Minimac3[52] (1.0.13) with the same reference panel used for the GWAS. For replication purposes, we allowed Rsq ≥ 0.5 throughout the study.

To investigate the X chromosome, we called genotype using BeadStudio. First, we

generated genoplot using only female. After that, we added male samples to genoplot and called genotypes. Genotypes called as heterozygote were treated as missing in male. For the genotype QC, we excluded variants with a MAF < 0.05 % and a variant call rate ≤ 0.99 in either male or female. We also excluded variants with *P*-value for Hardy–Weinberg equilibrium ≤ 1.0×10^{-6} in female. Haplotype phasing and imputation were performed separately for males and females in the GWAS. Allelic dosage were imputed from 0 to 2 in male under the assumption of full dosage compensation. In the population based-cohorts, pre-phasing was performed for males and females together using SHAPEIT, and the data were imputed separately. The pseudo-autosomal region was excluded from the reference before imputation.

Association analyses

The GWAS was performed using imputed allele dosages and fitted to an additive genetic model by mach2qtl[52]. We performed a stepwise conditional analysis to determine independent association signals near associated loci (lead variants ± 1Mb) using samples included in the GWAS until the top associated variants fell below the GWS level in each step-wise procedure. Meta-analysis was performed using the inverse-variance method under the assumption of the fixed effect model. Heterogeneity between studies and *P* for difference in the stratified analyses were calculated by Cochran's Q test. To investigate associations of the variants on X chromosome, we performed association analyses using mach2qtl in male and female, respectively. After that, we integrated the results of each sex by inverse-variance method under the assumption of the full dosage compensation.

We estimated the variance explained by each identified variant using the following formula using the allele frequency (*f*) estimated in the GWAS and estimates of the additive effect (β) in meta-analysis: $\text{Explained variance} = \beta^2(1-f)2f$. To estimate the additive

explained variance of 83 independent lead variants of identified loci, the explained variance of each individual variant was summed.

R (ver. 3.1.3) was used for these analyses. Regional association plots were generated by Locuszoom[54] (ver.1.3) and R.

Estimation of biases in the GWAS using LD score regression

To evaluate biases resulting from population stratification and cryptic relatedness, we performed LD score regression[15] with the default settings. LD scores for the East Asian population provided with software was used.

Sex-stratified GWAS

For the sex-stratified GWAS, the samples analyzed in the GWAS were divided by sex. We recalculated phenotypes in each sex stratum using residuals calculated by linear regression analysis using age, age^2, status of diseases, and the top 10 PCs as covariates. For the evaluation in the replication sets (population-based cohorts), we selected variants at each locus that showed $P < 1.0 \times 10^{-6}$ unless loci showed this level of association in the primary GWAS. As a result, we selected 12 variants for males and 3 variants for females.

T2D stratified analysis

We selected 31,609 individuals with T2D from samples analyzed in the GWAS. Individuals with type 1 diabetes, maturity-onset diabetes of the young, mitochondrial diabetes, and gestational diabetes were excluded from this analysis. We analyzed 193 lead variants of the loci reached genome-wide significant level. In case the lead variants were differed between Japanese only analysis and trans-ethnic analysis, we choose lead variants found in the Japanese GWAS. The BMI phenotype was re-evaluated from the residuals calculated by a

linear regression analysis using age, age^2, sex, status of 46 diseases, and the top 10 PCs after stratification. We tested association for T2D susceptibility using logistic regression analysis with 10 PCs as covariates.

Trans-ethnic meta-analysis

To carry out a meta-GWAS using our GWAS and publicly available result of Europeans[6] which was conducted by GIANT consortium, we downloaded the summary statistics from their website. After adding the positional information using the HapMap project phase2 to the summary statistics of the GIANT consortium, chromosomal position was converted to hg19 by the lift-over tool. We excluded the variants which were duplicated, and without allele frequency information, and included the variants which were analyzed in the both studies. Finally, we analyzed 2,078,865 autosomal variants in this study. We also conducted the meta-analyses of the sex-stratified GWASs in the same way.

For the meta-analyses, we used MANTRA[19] (v2) software which was designed for trans-ethnic meta-analysis with allowing heterogeneity in allelic effects. Prior model of the relatedness between the studies was estimated by dmatcal script in the software using the allele frequency of the analyzed variants. We considered $\log_{10}BF > 6$ as a significant threshold according to the previous simulation study[20]. To compare with result of the fixed effect model, we also performed meta-analysis using inverse variance method, and estimated heterogeneity using Cochran's Q test only for the significant loci.

Credible sets

Using the results from the trans-ethnic meta-analyses, we constructed the set of the variants which are likely to be causal based on the MANTRA[19] analysis. For the each locus, we considered the window which was determined by position of the lead variants ± 500 kb,

and calculated the posterior probability (PP) of the causal variant for the j_{th} variant under the assumption of a single causal variant in each locus using the following formula:

$$\mathrm{PP}_j = \frac{BF_j}{\sum_k BF_k}$$

where *k* denotes the variants in the window. After that, we selected the smallest set of variants to account for more than or equal to 99% of the PP in each locus.

Genetic correlation

To estimate the genetic correlations, bivariate LD score regression[16] was conducted using the results from the current GWAS of all samples, the GWASs of 33 complex diseases, and the hematological traits with the LD scores for the East Asian population (**Supplementary note**). All the GWASs that were analyzed only included Asians. We calculated the false discovery rate using the Benjamini–Hochberg procedure.

GREML analysis

To estimate the variance explained by autosomal variants, we selected imputed variants with Rsq ≥ 0.7 and generated a genetic relatedness matrix (GRM) for the Japanese cohorts by GCTA (ver. 1.25)[26]. For the GREML analysis, we used samples whose genetic relationship was less than 0.05. Then, 5,612 and 6,434 samples in the JPHC and the TMM, respectively, were included in these analyses. The log-transformed BMI values were then standardized to be Z-scores adjusted for age, age^2, and sex in each cohort. Explained variance was estimated using the reml function implemented in GCTA software with default settings. We also estimated the variance explained by each chromosome using the reml function and the “--reml-no-constrain” option. The X chromosome was analyzed under the assumption that there was full dosage compensation in females. We calculated weighted averages from results of two cohorts using inverse-variance weighting. In the regression

analysis for chromosome length, negative values were constrained at zero after calculation of weighted averages.

Pleiotropy

We downloaded the NHGRI GWAS catalog on Feb 19, 2016. We converted chromosomal positions from hg38 to hg19 using the liftOver tool in the UCSC genome browser. To prioritize other reported traits, we manually selected variants that satisfied one of the following criterion for each identified variant from the GWAS catalog: 1) variants with $r^2 \geq 0.5$ in East Asians if the publication included Asians, 2) variants with $r^2 \geq 0.5$ in both East Asians and other population if the original report not studied East Asian, and 3) the physical distance from lead variants in the present GWAS to variants reported in the GWAS catalog was within 25 kb. LD was calculated according to 1KGP.

Tissue-specific active enhancer enrichment

To investigate cell-types and cell-groups which are relevant to obesity, we conducted an enhancer enrichment analysis using variants included in the 99% credible sets constructed by trans-ethnic meta-analysis. Since there are several types of enhancer information, we annotated the variants included in the trans-ethnic GWAS, and compared the overlaps of three different types of enhancers (15 state model: state 7, 18 state model: state 9, and DNaseI-accessible enhancer) in each cell-types. We observed that active enhancer in the ChromHMM 18 state model (state 9) shows lowest overlaps across cell-types among analyzed enhancers (**Supplementary Note**). Therefore, we determined to use active enhancer of ChromHMM 18 state model for this analysis.

For the cell-type and cell-group specificity analysis, we excluded the cell-types which are derived from cell-lines, labeled as cultured cell, and belonging to ESC or iPSC

groups. To test statistical significance, we compared the overlaps between variants in the 99% credible sets and the same number of randomly selected ones from the background variants which are locate at position of the lead variants ± 500 kb and not selected in the credible sets. To avoid bias resulting from allele frequency differences, we controlled MAF in EAS and EUR for the background variants with variants in the credible sets by dividing MAF into four categories for each population (1: MAF < 5%, 2: 5% < MAF ≤ 15%, 3: 15% < MAF ≤ 30%, 4: MAF > 30%) in each permutation procedure. We calculated empirical *P* value by 10^7 permutations using R. FDR was estimated by Benjamini–Hochberg method.

Tissue-specific H3K4me3 enrichment

To evaluate overlaps of tissue-specific H3K4me3 at 85 identified autosomal variants, we used epiGWAS software[24]. We calculated LD (r^2 cutoff = 0.8) between the lead variant and variants within 500kb window using computeLD.py script in the software with LD information from the EAS samples in 1KGP. We analyzed the H3K4me3 peaks of 34 tissues obtained from the Roadmap project, which was included in the software. To estimate the statistical significance of cell-type-specific overlaps, 10^6 permutations were performed. The H3K4me3 peaks were shown in a regional association plot (**Supplementary Data Set 1** and **2**). We also analyzed 97 variants reported by GIANT consortium in the same way using LD information of the EUR samples in 1KGP.

Functional annotation and eQTL analysis

For the annotation of the nonsynonymous variant, ANNOVAR[55] was used. We annotated the variants with enhancer information using bedtools (v2.17.0).

To evaluate the overlaps between GWAS signal and cis-eQTL, we annotated the lead variants found in the trans-ethnic meta-analysis. We targeted the tissues which were

genetically suggested its involvement by our cell-type specificity analyses. To prioritize eQTLs, we used GTEx[24] (Release v6) and whole-blood eQTL information[25]. These data were downloaded from their website. We set significant threshold for eQTL as FDR < 0.05. In each datasets, we only considered the variants which were analyzed in our trans-ethnic analysis, and selected the variants which showed strongest association for each transcript. We regarded significant overlap if the GWAS lead variant was in LD ($r^2 \geq 0.8$) in EUR samples of 1KGP with lead variant of the eQTL.

Pathway analysis

We used MAGENTA[28] for pathway analysis. Genes in the HLA region were excluded from the analysis. To adapt the LD structure of East Asians, we pruned the variants in EAS samples of 1KGP using the '--indep-pairwise' option of PLINK[51]. Default parameters were applied for other settings. We regarded the pathways that showed a FDR $q < 5\%$ as significant.

Data availability

The genotype data, BMI measurements, and related phenotype information that support the findings of this study are available in Japanese Genotype-phenotype Archive (JGA; http://trace.ddbj.nig.ac.jp/jga/index_e.html) with the accession codes: JGAS00000000114 for the study, JGAD00000000123 for the genotype data, and JGAD00000000124 for the BMI measurements, respectively. The summary statistics of the GWAS have been deposited in the National Bioscience Database Center (NBDC) Human Database (https://humandbs.biosciencedbc.jp/en/) with the Data Set ID (hum0014.v6.158k.v1).

Methods-only references

50) Price, A. L. et al. Principal components analysis corrects for stratification in genome-wide association studies. *Nat. Genet.* **38**, 904–9 (2006).

51) Purcell, S. et al. PLINK: a tool set for whole-genome association and population-based linkage analyses. *Am. J. Hum. Genet.* **81**, 559–75 (2007).

52) Li, Y., Willer, C. J., Ding, J., Scheet, P. & Abecasis, G. R. MaCH: using sequence and genotype data to estimate haplotypes and unobserved genotypes. *Genet. Epidemiol.* **34**, 816–34 (2010).

53) Delaneau, O., Marchini, J. & Zagury, J.-F. A linear complexity phasing method for thousands of genomes. *Nat. Methods* **9**, 179–81 (2012).

54) Pruim, R. J. et al. LocusZoom: regional visualization of genome-wide association scan results. *Bioinformatics* **26**, 2336–7 (2010).

55) Wang, K., Li, M. & Hakonarson, H. ANNOVAR: functional annotation of genetic variants from high-throughput sequencing data. *Nucleic Acids Res*. **38**, e164 (2010).

Figure 1

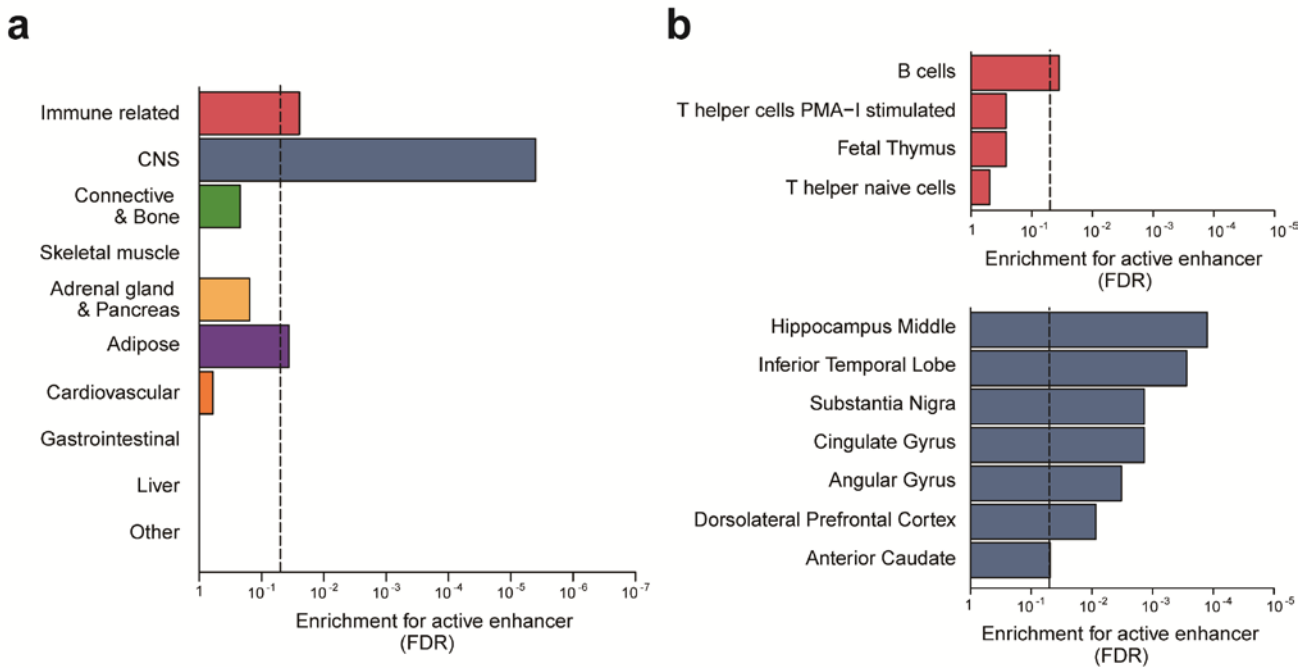
a
Immune related
CNS
Connective & Bone
Skeletal muscle
Adrenal gland & Pancreas
Adipose
Cardiovascular
Gastrointestinal
Liver
Other
1
10-1
10-2
10-3
10-4
10-5
10-6
10-7
Enrichment for active enhancer (FDR)
b
B cells
T helper cells PMA−I stimulated
Fetal Thymus
T helper naive cells
Enrichment for active enhancer (FDR)
Hippocampus Middle
Inferior Temporal Lobe
Substantia Nigra
Cingulate Gyrus
Angular Gyrus
Dorsolateral Prefrontal Cortex
Anterior Caudate
Enrichment for active enhancer (FDR)

Figure 2

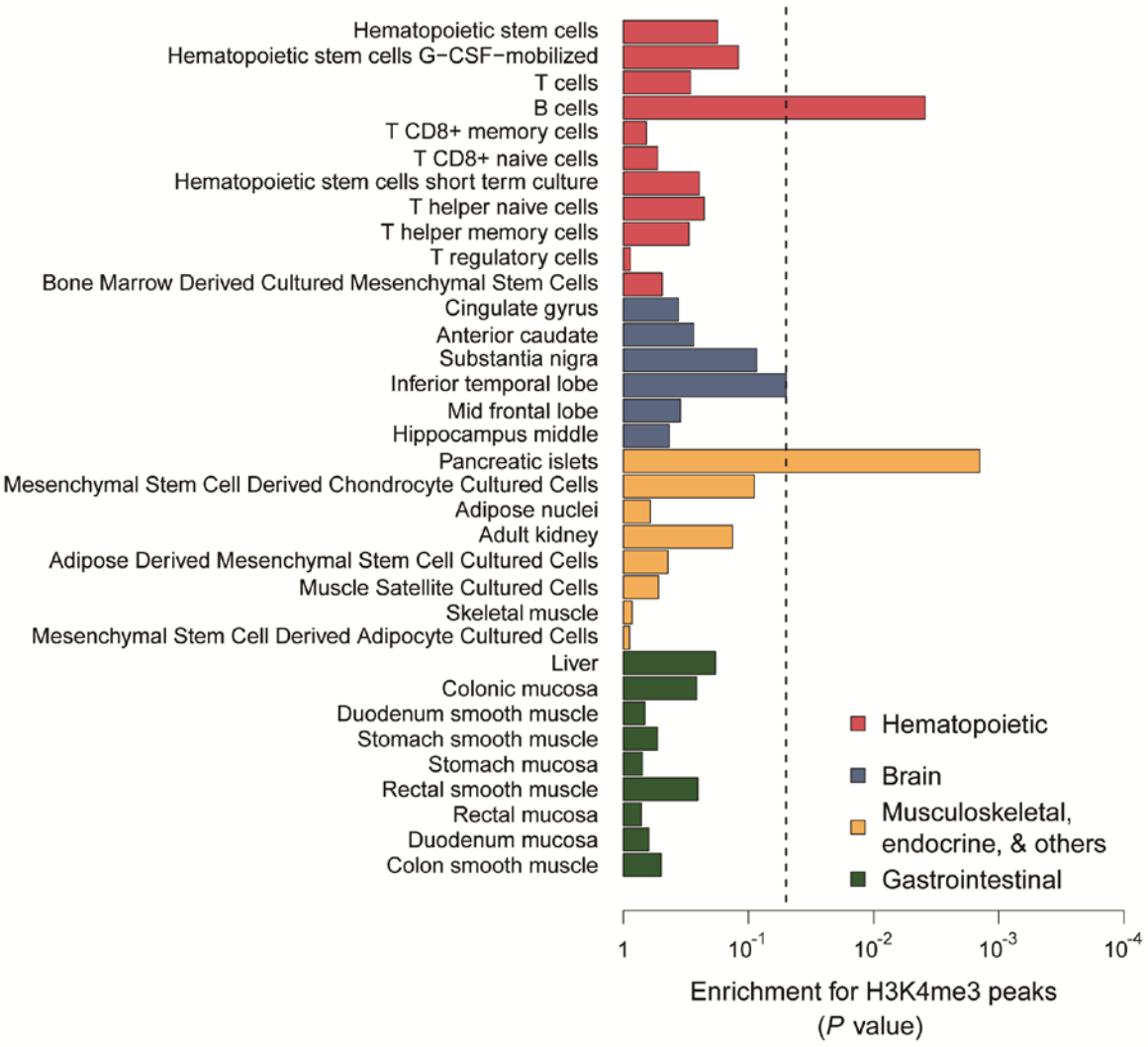
Hematopoietic stem cells
Hematopoietic stem cells G−CSF−mobilized
T cells
B cells
T CD8+ memory cells
T CD8+ naive cells
Hematopoietic stem cells short term culture
T helper naive cells
T helper memory cells
T regulatory cells
Bone Marrow Derived Cultured Mesenchymal Stem Cells
Cingulate gyrus
Anterior caudate
Substantia nigra
Inferior temporal lobe
Mid frontal lobe
Hippocampus middle
Pancreatic islets
Mesenchymal Stem Cell Derived Chondrocyte Cultured Cells
Adipose nuclei
Adult kidney
Adipose Derived Mesenchymal Stem Cell Cultured Cells
Muscle Satellite Cultured Cells
Skeletal muscle
Mesenchymal Stem Cell Derived Adipocyte Cultured Cells
Liver
Colonic mucosa
Duodenum smooth muscle
Stomach smooth muscle
Stomach mucosa
Rectal smooth muscle
Rectal mucosa
Duodenum mucosa
Colon smooth muscle
Hematopoietic
Brain
Musculoskeletal, endocrine, & others
Gastrointestinal
1
10-1
10-2
10-3
10-4
Enrichment for H3K4me3 peaks
(P value)

Figure 3

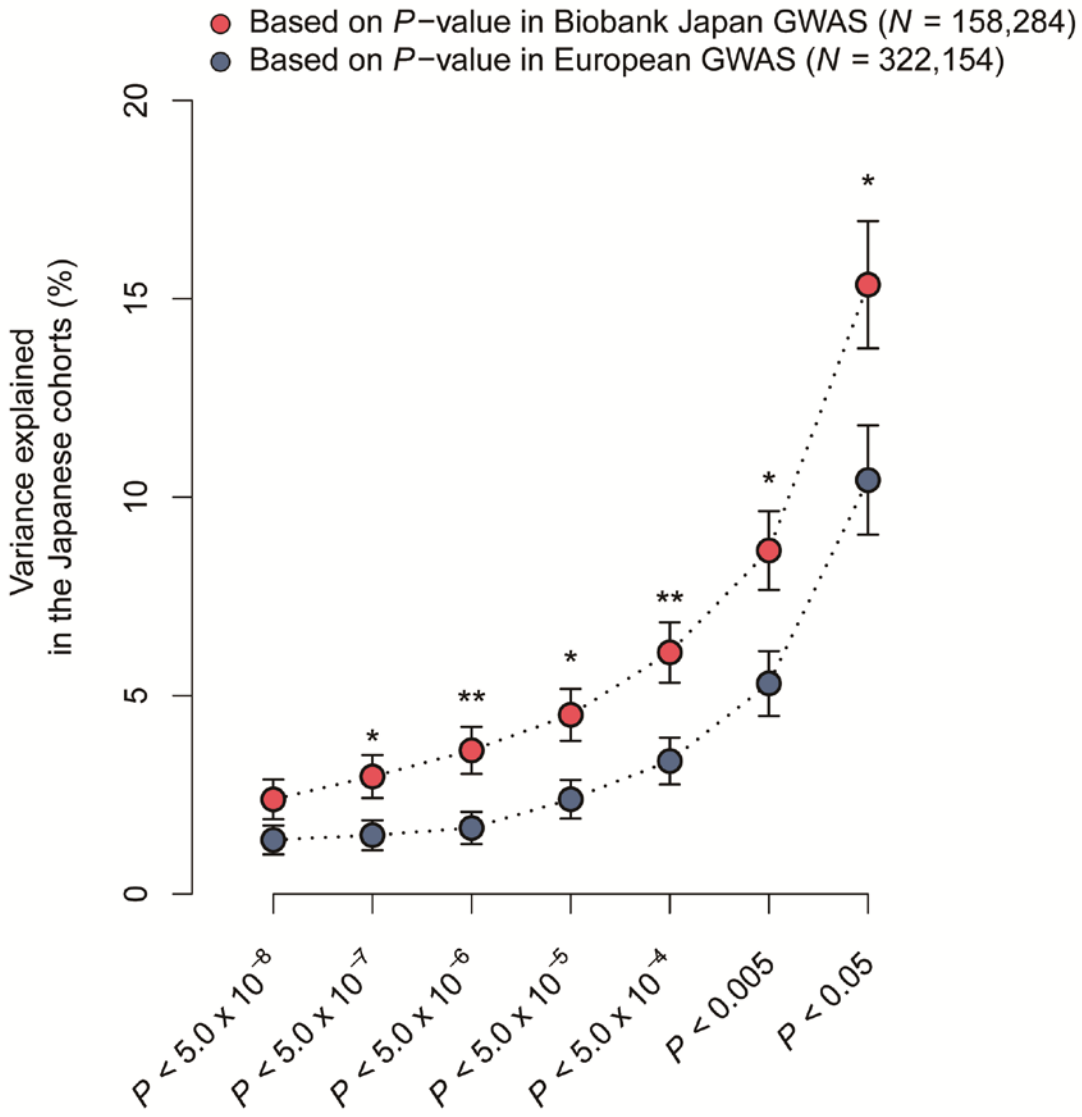
Based on P−value in Biobank Japan GWAS (N = 158,284)
Based on P−value in European GWAS (N = 322,154)
Variance explained in the Japanese cohorts (%)
0
5
10
15
20
*
**
*
**
*
*
P < 5.0 x 10−8
P < 5.0 x 10−7
P < 5.0 x 10−6
P < 5.0 x 10−5
P < 5.0 x 10−4
P < 0.005
P < 0.05

Figure 4

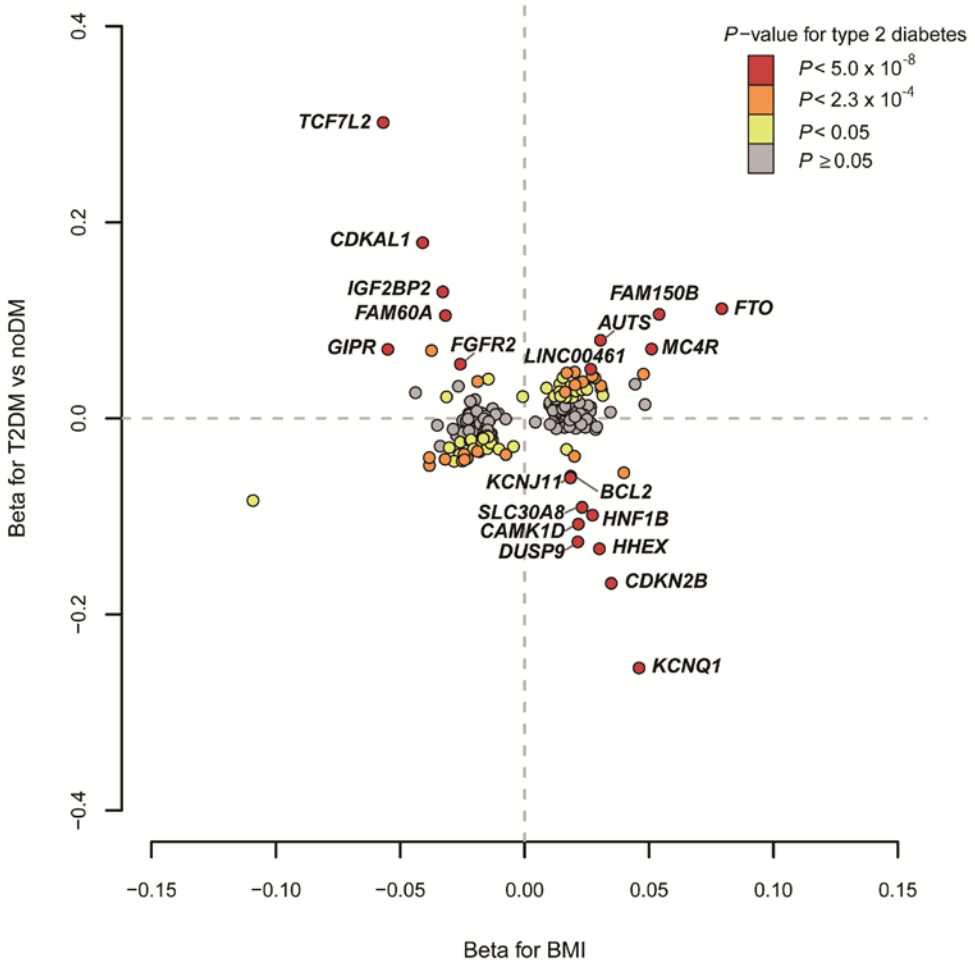
P−value for type 2 diabetes
P< 5.0 x 10-8
P< 2.3 x 10-4
P< 0.05
P ≥0.05
TCF7L2
CDKAL1
IGF2BP2
FAM60A
GIPR
FGFR2
FAM150B
AUTS
FTO
MC4R
LINC00461
KCNJ11
BCL2
SLC30A8
HNF1B
CAMK1D
DUSP9
HHEX
CDKN2B
KCNQ1
Beta for T2DM vs noDM
Beta for BMI
0.4
0.2
0.0
−0.2
−0.4
−0.15
−0.10
−0.05
0.00
0.05
0.10
0.15

Figure 5

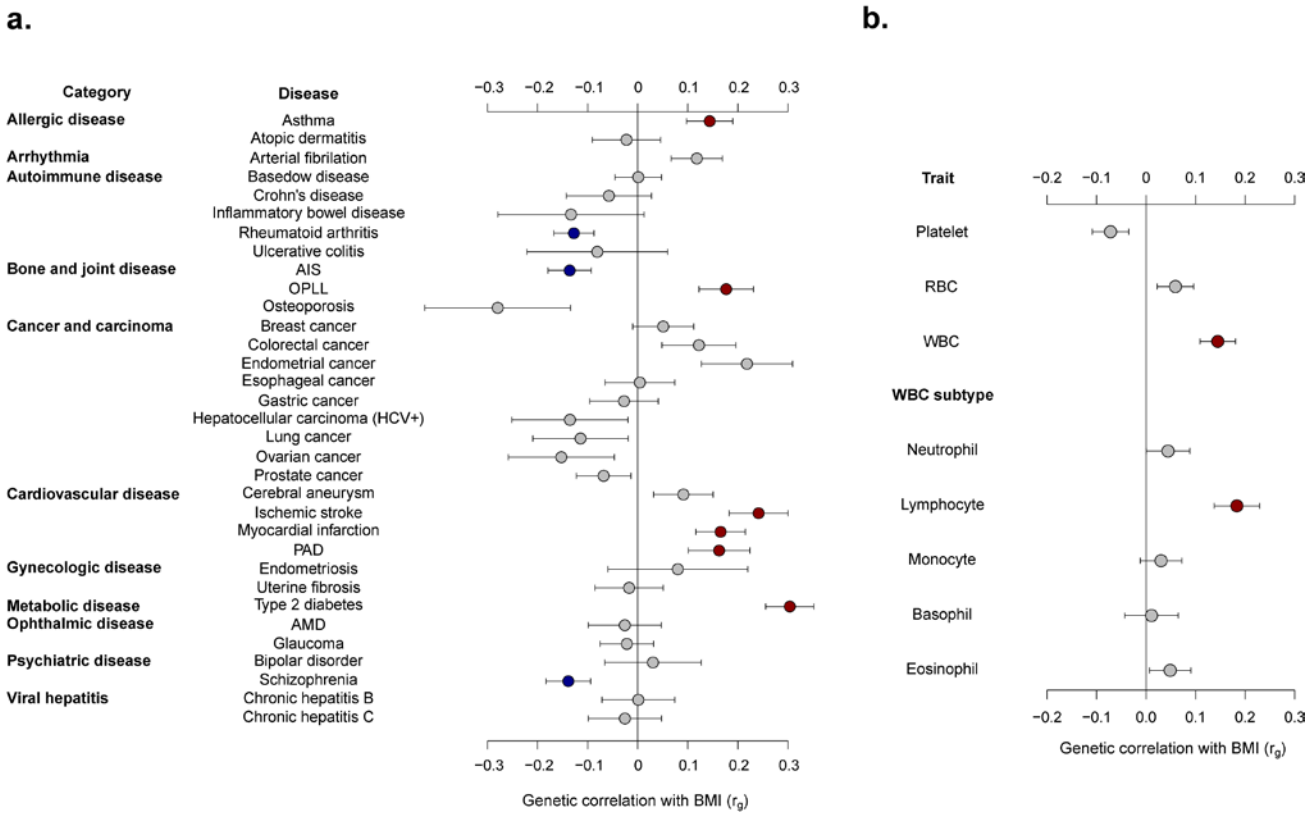
a.
Category
Disease
Allergic disease
Asthma
Atopic dermatitis
Arrhythmia
Arterial fibrilation
Autoimmune disease
Basedow disease
Crohn's disease
Inflammatory bowel disease
Rheumatoid arthritis
Ulcerative colitis
Bone and joint disease
AIS
OPLL
Osteoporosis
Cancer and carcinoma
Breast cancer
Colorectal cancer
Endometrial cancer
Esophageal cancer
Gastric cancer
Hepatocellular carcinoma (HCV+)
Lung cancer
Ovarian cancer
Prostate cancer
Cardiovascular disease
Cerebral aneurysm
Ischemic stroke
Myocardial infarction
PAD
Gynecologic disease
Endometriosis
Uterine fibrosis
Metabolic disease
Type 2 diabetes
Ophthalmic disease
AMD
Glaucoma
Psychiatric disease
Bipolar disorder
Schizophrenia
Viral hepatitis
Chronic hepatitis B
Chronic hepatitis C
−0.3 −0.2 −0.1 0 0.1 0.2 0.3
Genetic correlation with BMI (r_g)
b.
Trait
Platelet
RBC
WBC
WBC subtype
Neutrophil
Lymphocyte
Monocyte
Basophil
Eosinophil
−0.2 −0.1 0 0.1 0.2 0.3
−0.2 −0.1 0.0 0.1 0.2 0.3
Genetic correlation with BMI (r_g)